MULTISCIA
JOURNALS PUBLISHERS

FRONTIERS IN MECHANICAL, MINING AND MATERIAL ENGINEERING

ISSN: (3065- 4025)

https://multisciajournals.com/journals/index.php/fmmme

editor.fmmme@gmail.com

Frontiers in Mechanical, Mining and Material Engineering
Volume 1 Issue 3 2025

IMPACT OF INITIAL MICROSTRUCTURE ON THE CARTRIDGE CASE EARRING OF ALUMINIUM ALLOYS

Ahmad , Aamir H. Bhatia

Depatment of Mech

Article Info

Received: 24-07-2025 ***Revised:02-09-2025*** ***Accepted:10-09-2025*** ***Published:20-09-2025***

Abstract

Investigations were conducted into defects discovered during the impact extrusion of EN AW-5754 aluminum alloy during the manufacturing of cartridge cases. There was a noticeable propensity to earring after impact extrusion in cartridge casings made from a single metallurgical heat. The earring in cartridge casings from the opposite heat, however, was not seen. The local variation in material flow during extrusion is what causes the presence of the earring. The variation in second phase particle distribution in utilized preforms (slugs) is the cause of this behavior.

Keywords: cartridge case; impact extrusion; earring; EN AW-5754 aluminiumalloy.

Introduction

Impact extrusion is regarded as a high-volume manufacturing process. The slugs are forcefully compressed between the die and punch during this procedure. Thin-walled, light-weight cylinders are created when material flows via reverse extrusion, allowing for significant deformation at high speed. When the cylinder's base is thicker than its side walls and the wall length is more than double its diameter, this method works better than deep drawing. While deep drawn items are usually restricted to a 1:1 wall/bottom ratio and a 2:1 length/width ratio, aluminum alloys may achieve length/width ratios of up to 8:1 and steel up to 4:1 in a single process. Impact extrusion may produce a cylinder with a thinner wall and significantly tighter tolerances than forging. Metal flow during the forming process is influenced by process variables including temperature, forming rate, and lubrication, which includes friction between the tooling and slug ·⁝·2–3⁝. But material qualities also need to be taken into account. Microstructural factors and mechanical attributes like strength and ductility are linked to formability.such as work hardening, dynamic recovery, solute, strengthening, particle hardening, grain size and texture □4-5□. The microstructure homogeneity is the most important for formability □6□. Due to the differences in material flow, which can be caused by listed parameters, the earring is quite common during impact extrusion. It is well known that the main reason which causes earring are anisotropic characteristics of the blank sheet which has crystallographic texture □7□. However, the slugs sawn from the drawn bars are often used as a preform for production of cartridge cases by impact extrusion. It is considered that the drawn rod having a grain pattern in the direction of extrusion and grain flow during impact extrusion would result in optimum macrostructure and strength of the material [8]. There is no data about the effect of texture in the drawn rod on earring during impact extrusion.

This study aimed to establish the relationship between the initial properties of the slugs and earring formation during impact extrusion of the EN AW-5754 alloy.

Experimental

Two cartridge cases of EN AW-5754 alloy were tested. The cartridge cases were produced from slugs, □42,8x12 mm, from different metallurgical heats, which chemical compositions are given in Table 1.

Table 1. The chemical composition of EN AW-5754 alloy slugs, wt. %

Slug	Mg	Mn	Si	Fe	Cu	Cr	Zn	Ti	Al
1	2.72	0.26	0.085	0.19	0.044	0.025	0.057	0.019	Bal.
3	2.87	0.29	0.16	0.36	0.046	0.048	0.057	0.017	Bal.

The slugs were sawn from extruded rods from two metallurgical heats (marked as 1 and 3). Slugs in as received condition were formed into cartridge cases by backward impact extrusion (Fig. 1).

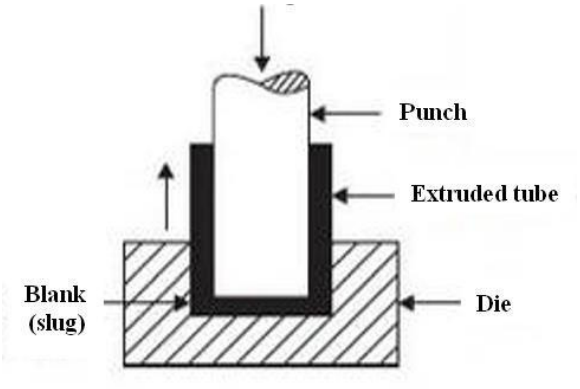

Fig. 1. Schematic illustration of the impact extrusion process.

Microstructure

A Leitz optical microscope and a scanning electron microscope (SEM-JEOL JSM-6610LV) were used to analyze the microstructure. Traditional methods, such as mechanically grinding with sandpaper and mechanically polishing with diamond paste up to 1 μm grade, were used to produce the metallographic samples. Following electrolytic polishing in perchloric acid, the samples were etched in Barker's solution (25 ml HBF4 (40%), 1000 ml distilled water) to disclose the grain structure. While samples of cartridge cases were cut as shown in Fig. 2 (pick-P, with the maximum height of 38,70 mm, and valley-V, with the lowest height of 34,28 mm), the particle distribution in polished samples was observed in the longitudinal and transverse direction of slugs.

Hardness measurement

Hardness measurements of slugs were conducted by the Brinell method according to standard SRPS EN ISO 6506-1, HB2,5/62,5. The hardness of the cartridge case was measured by Vickers method, under test force of 4.9 N, according to standard SRPS EN ISO 6507-1.

Electrical conductivity

Electrical conductivity measurements were performed on slugs using Föerster Sigma Test D2.068 equipment at the operating frequency of f=60 kHz.

Results

The geometry of cartridge cases

The tested cartridge cases are shown in Fig. 2. It can be seen that the uneven edge of the cartridge case 3, i.e., in the specimen 3 earring occurred after backward impact extrusion.

Fig. 2. Cartridge cases without (1) and with earrings (3).

The results of wall height measurement (conducted on 11 measuring places) of both cartridge case are given in Table 2, where h_{min} is the minimal height at the valleys, h_{max} the maximal height of the earring peaks, and Δh the difference (h_{max}-h_{min}). The results showed that Δh was 1.1 mm and 4.42 mm at cartridge case 1 and 3, respectively.

Table 2. Wall height of the cartridge cases, mm.

Measuring point	1	2	3	4	5	6	7	8	9	10	11
Cartridge case 1	-	-	37.4	37.0	36.7	36.8	37.0	37.3	37.8	37.8	37.8
Cartridge case 3	34.3	38.4	38.1	36.8	36.2	37.6	38.7	38.7	38.3	37.4	38.1

Table 3. Maximal and minimal wall height of the cartridge cases, mm.

Height	Cartridge case 1		Cartridge case 3	
h_{max}	37.85		38.70	
h_{min}	36.75		34.28	
Δh		1.10		4.42

At the same time measurement of the wall thickness of cartridge cases show that the wall thickness is quite uniform.

Microstructure

The microstructure of the slugs is shown in Fig. 3. Grain structure analysis revealed recrystallized microstructure with slightly elongated grains in the longitudinal direction of both slugs. The difference between the grain size of specimens can be neglected.

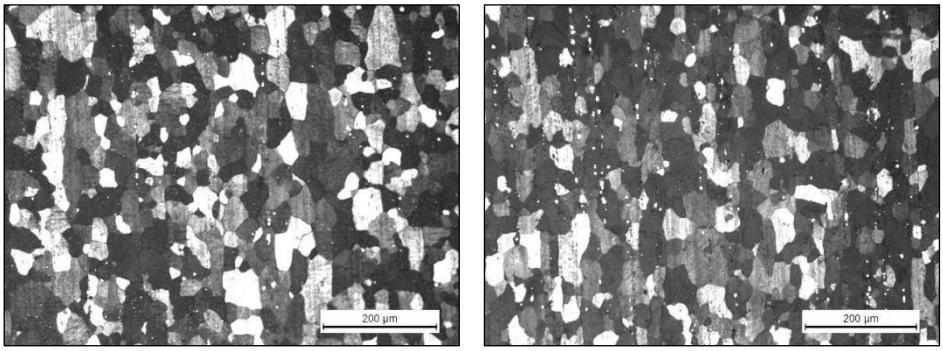

a) *b)*

Fig. 3. Grain structure in the longitudinal section of slugs 1 and 3; etched.

Particle distribution of the slugs observed with a light microscope and SEM is shown in the Figs 4 and 5. It was noted the stringer-like distribution of second phase particles in the longitudinal direction of both slugs. Higher content of the second-phase particles was observed in the slug 3 than in the slug 1. This is also confirmed at the microstructures in the cross section (Figs. 5a and 5b). The second-phase particles in the cross section of the slugs were found to be randomly distributed in both specimens, but larger particles were identified in slug 3.

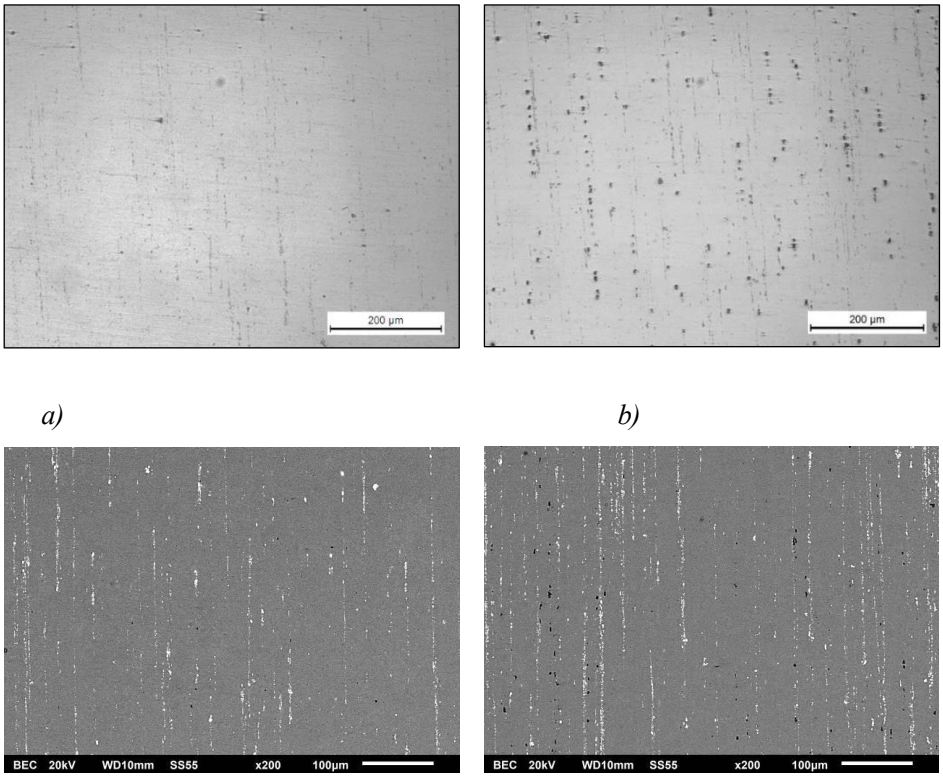

a) *b)*

c) *d)*

Fig. 4. Particle distribution in the longitudinal direction of: a), c) slug 1; b), d) slug 3; a), b) LM; c), d) SEM.

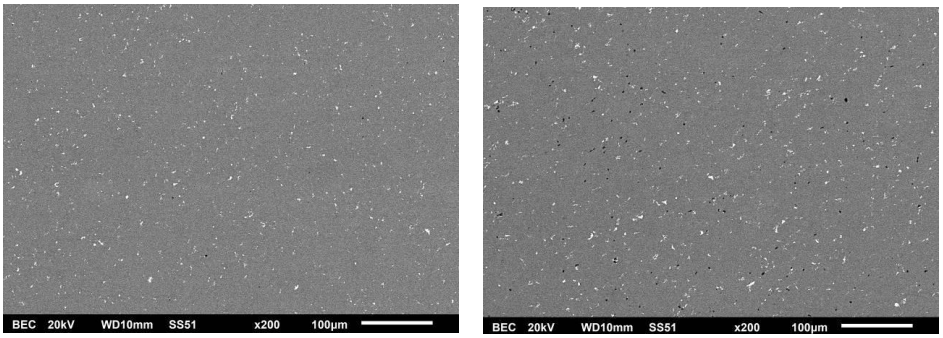

a) *b*

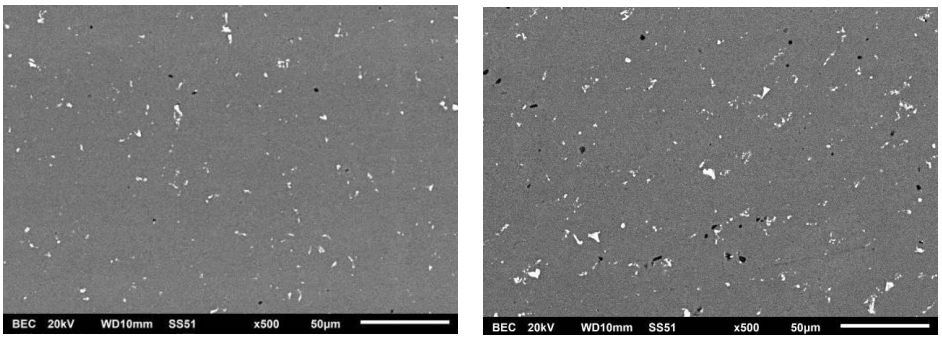

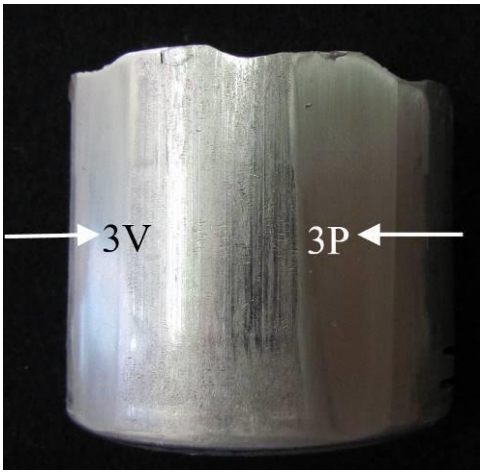

c) *d)Fig. 5. Particle distribution in the cross-section of the slugs 1 and 3.*

Fig. 6. Specimen for testing microstructure and microhardness of the cartridge case 3. V-valley and P-peak areas.

Microstructures of the wall surface of the cartridge case 3 in the area of the valley (h_{min}), and peak (h_{max}) (Fig. 6) are shown in Fig. 7. The clear difference in second phase particles content of valley and pick area in the wall surface was observed (Fig. 7). From the micrograph given at Figs 7a and c, it seems that in the valley area a larger number of particles could be observed.

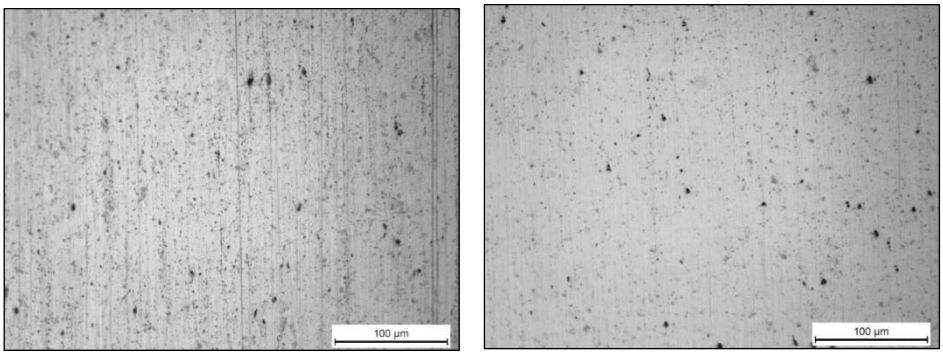

a) *b)*

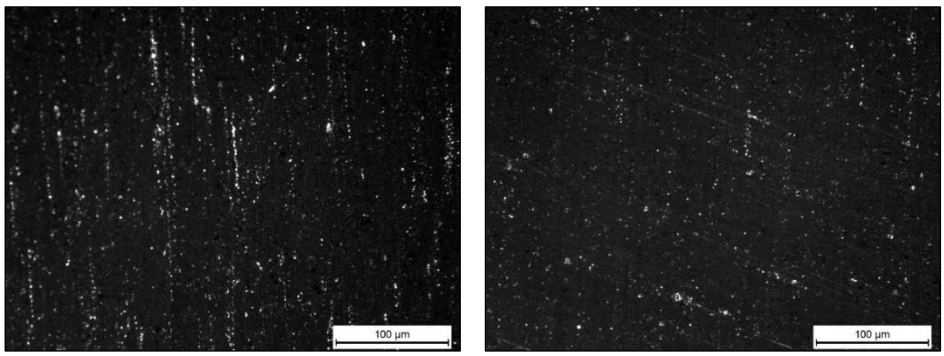

c) *d)*

Fig 7. Particle distribution in the wall surface of the cartridge case 3: a), c) valley; b), d) peak. Polished. a), б) bright field; c), d) dark field.

The second phase particles have been identified by EDS as Al-Fe-Mn(Ni) (white in BS images) and Mg-Si phases, as shown in Fig. 8. Other particles (Al-Mg-Fe, Al-Mg), were also observed. According to [9-11], the light coarse particles which dominated in microstructures were identified as (Fe, Mn)Al6.

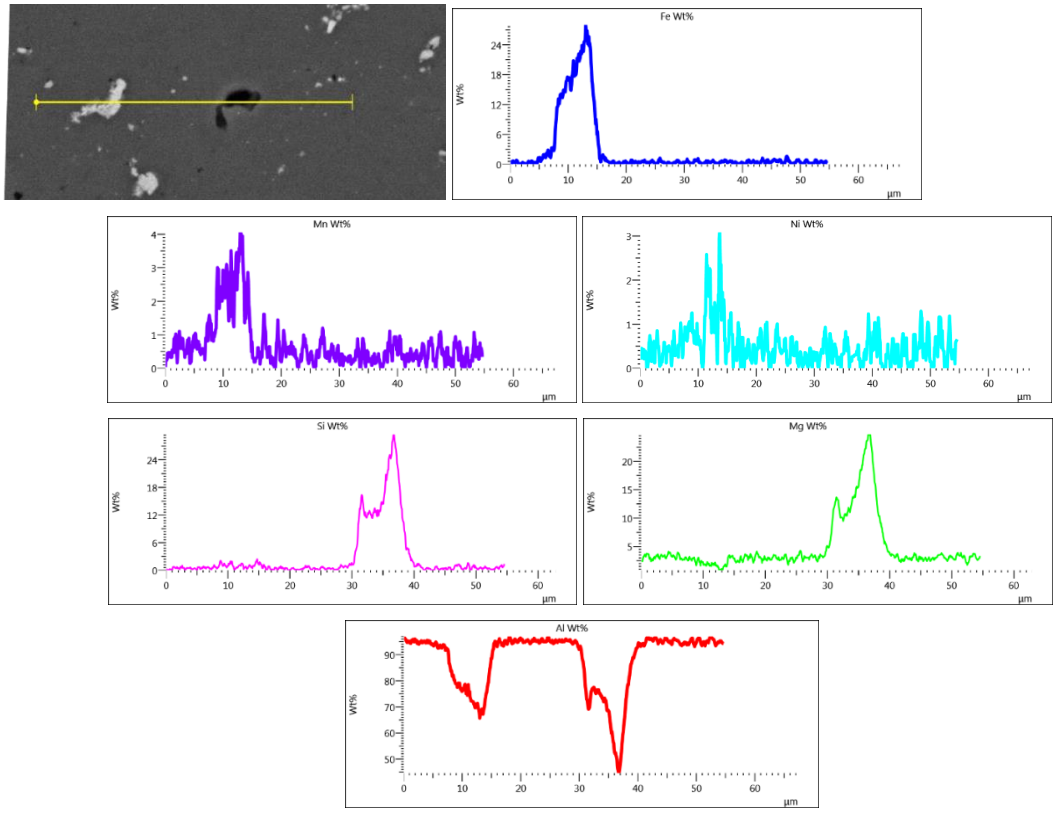

Fig. 8. EDS of second phase particles in EN AW-5754 alloy.

Hardness

Results of hardness measurement are given in Table 4. It was found that the hardness of the slug 3 is slightly higher compared to the hardness of the slug 1.

Table 4. The hardness of the slugs 1 and 3.

Specimen		HB		Aver.
Slug 1	59.0	58.0	57.7	58
Slug 3	61.4	61.0	59.4	61

The hardness of the cartridge case 3, measured in circumference (Fig. 6) is given in Table 5. It was found that the hardness of the valley area (V) is higher compared to the wall pick area (P).

Table 5. Wall hardness of the cartridge case 3.

Specimen		HV0.5		Aver.
3 P	104.6	102.5	104.1	104
3 V	112.0	112.9	114.4	113

Electrical conductivity

Results of electrical conductivity measurements are given in Table 6. Lower values of electrical conductivity were measured in the slug 3.

Table 6. The electrical conductivity of the slugs.

Specimen	Electrical conductivity, %IACS					Aver.
Slug 1	34.67	34.57	34.55	34.66	34.55	34.60
Slug 3	33.71	33.69	33.74	33.74	33.69	33.71

Discussion

Two metallurgical temperatures were used to create the cartridge casings. They were discovered to have slightly distinct characteristics. With a larger concentration of alloying elements and impurities, including Mg, Mn, Fe, Si, and Cr, Slug 3 was created using metallurgical heat (Table 1). Significant impurity levels are often seen in aluminum alloys, which cause second phase particles to develop. Fe is thought to be the primary contaminant that creates the Fe-rich intermetallic ·⁚·12–13⁚ in Al–Mg based alloys. Microstructure analysis verified that slug 3's greater amount of alloying elements and contaminants led to the production of bigger and more abundant second phase particles (Figs. 4 and 5). As a consequence, the hardness value increased (Table 4). It is well known that various microstructural characteristics of Al-Mg alloys may be detected with great sensitivity using the electrical conductivity of these alloys. As alloying elements and contaminants rise, electrical conductivity diminishes (14–16). According to the findings of chemical composition, as well as hardness and microstructure (Table 1 and 4, Figs. 4 and 5), the electrical conductivity of the slug 3 (Table 6) is lower than that of the slug 1. It is well known that aluminum alloys have a very non-homogeneous second phase particle distribution □17□. Larger and smaller regions are identified in this investigation because the second phase particle distribution in cartridge case 3 was somewhat non-homogeneous (Fig. 6). The valley (V) region has the highest concentration of second phase particles (Fig. 6a, c).As a consequence, after impact extrusion, the cartridge wall's circle had an uneven distribution of hardness. According to Table 5, the hardness of the valley (V) is greater than that of the wall pick (P) region. Both non-homogenous second phase distribution and non-homogenous strengthening during cold deformation (impact extrusion) contribute to this hardness dispersion. The rate of deformation strengthening is greater in a region with a larger concentration of second phase particles (valley wall) [18–19].

Simultaneously, measurements of cartridge case wall thickness reveal that the wall thickness is quite consistent. We may infer that the backward extrusion technique offers superior control over the thickness of the sidewall.

In conclusion

Backward impact extrusion was used to create the cartridge casings from slugs. The two examined slugs, which were made using different metallurgical temperatures, were discovered to have somewhat different chemical compositions. It was also discovered that the examined slugs made from various metallurgical temps had variable mechanical, physical, and microstructure characteristics.

Due to the somewhat greater level of impurities (Fe, Si, and Cr) and alloying elements (Mg), more second phase particles were found in slug 3 than in slug 1. Furthermore, slug 3 has a more uneven distribution of second phase particles. This slug's poorer electrical conductivity and increased hardness in comparison to Slug 1 are consistent with its microstructure and chemical makeup.

The earring was visible in cartridge casings made from the slug 3 after impact extrusion. The hardness varied throughout the sections of the various wall heights. The hardness of the wall picks is greater than that of the valleys. Additionally, the valley region has a larger concentration of second phase particles than the wall picks. These discrepancies result from the original slugs' second phase particles' non-homogeneous size and dispersion region. This led to the earring's non-homogeneous deformation, or the localized variation in material flow during the cartridge case's impact extrusion.
The sidewall thickness was well-controlled using the backward extrusion method.

References

[1] Impact Extrusion in Comparison to Other Methods, retrieved March 2019, from http://metalimpact.com/products capabilities/impact extrusion in comparison to other procedures.
[2] S.H. Kim, S.W. Chung, S. Padmanaban: J Mat Process Tech, 180 (2006) 185–192.
[3] Trans Nonferrous Met Soc China, 22 (2012) 48–53 in HU Cheng-liang, MENG Li-fen, ZHAO Zhen, GU Bing, and CAI Bing.

[4] Xiang-Ming Cheng, Aluminum alloys: structure, texture, and formability, University of Kentucky, 2000.
In J Mat Process Technol, 211(9) (2011) 1516-1526, S. Hazraa, D. Williamsa, R. Roya, R. Aylmoreb, and A. Smith are the authors.
[6] Plasticity-related_properties_069bc.pdf, http://ecampus.sriramanujar.ac.in/files/files_2015/Plastic Deformation of Metals and Related Properties
The impact of earring factors on aluminum alloy earrings, J Yekarum (2014) 16-19, K. Delikanli.
[8]Close-air-support gun system development program for 30mm aluminum alloy cartridge case, Technical report AFATL-TR-71-23, Eglin Air Force Base, Florida, 1971.
[9] Mater. Charact. 65 (2012) 16-27 E. Romhanji, M. Popović, and T. Radetić.
[10] L. F. Mondolfo, Aluminum Alloys: Structure and Properties, Butterworths, Boston, 1976.
[11] Lj. Radović FTN Čačak, Deformacion ponašanje i karakteristike loma Al-Mg legura u svetlu međuzavisnosti sastav-tehnologija-struktura, 2013.
[12] J.R. Davis, Understanding the Fundamentals of Aluminum and Aluminum Alloys in Alloying, Ed. J.R. Davis Davis & Associates, ASM International, Metals Park, Ohio (2001) 351-416.
[13] Journal of Alloys and Compounds 728 (2017) 669-681: O. Engler, K. Kuhnke, J. Hasenclever.
58 (2) (2008) 14-19; Lj. Radović, M. Nikačević: Sci Tech Rev.
[15] J. Nondestructr Eval, 29 (2010) 43–48; E. Romhanji, M. Popovic, S. Stanojević.
Y. Zhao, J.G. Morris, and W. Wen: Mat Sci Eng, A 392 (2005) 136–144.
[17] Z. Chen, Second phase particle distribution and its impact on aluminum alloy formability in Computational Methods and Experiments in Material Characterization II, edited by C.A. Brebbia and A.A. Mammoli, eISBN 978-1-84564-212-9, WIT Press 2005, 53-62.
[18] Prec Indian Acad Sci (Engg Sci), 3 (4) (1980) 275-296; S. V. Kailas.
[19] Prec Indian Acad Sci (Engg Sci) 3, (4) (1980) 275-296; T Balakrishna Bhat, V S Arunachalam.